Dynamic Response of Self-acting Foil Bearings

Abstract: A new approach to the analysis of wide foil bearings is investigated. The equation of motion for a finite length of tape is coupled to the transient lubrication equation for the air film between the tape and the recording head. Compressibility and slip flow are retained in the fluid mechanics equation; flexural rigidity and high-speed dynamic effects are retained in the tape equation. The steady-state solution to the coupled equations is obtained as the limiting case of the transient initial value problem. Describing the system equations relative to the undeflected tape (as opposed to conventional foil-bearing theory, which uses the head as the reference surface) permits investigation of noncircular head geometries. In addition, wave propagation effects in the tape and the interaction of waves in the tape with the air-bearing region may be studied.

Introduction

Development of digital magnetic recording devices using flexible media as the recording surface is dependent on accurate positioning of the recording element relative to the medium. The demands of high-density recording with a high data transfer rate require that the separation between head and medium be very small (<1.25 μ m) while the head-to-medium velocity must be large (>2.5 m/s, in some cases). To achieve these goals with reasonable longevity of the recording medium, a hydrodynamic air bearing can be used to provide a controllable separation of the head and medium with, in the ideal case, no contact between the two.

Although the configurations of flexible-media recording devices may be quite complicated, it is usually possible to formulate a system of equations that can be expected to adequately describe the elastohydrodynamic interaction of the device. Often the elasticity equations describing the motion of the medium, or the fluid mechanics equations describing the behavior of the air bearing, can be solved independently to obtain information about the system behavior. To predict the spacing between a head and a flexible medium requires the simultaneous solution of the coupled system of equations, however, and it is in this area that significant difficulties occur, because of the strong interaction of the system equations.

In recent years, a relatively large amount of literature [1-12] has been devoted to the solution of foil-bearing problems in which the flexible medium is wrapped around a circular cylinder. The elasticity equations describing the motion of the medium and the lubrication

equation for the air film are written in a coordinate system attached to the surface of the cylinder, following the derivation given by Barlow [1]. Thus, a tractable mathematical problem is obtained if the cross section of the cylinder be either circular or composed of circular arcs [5]. Otherwise, the mathematical difficulties inherent in the problem formulation prohibit convenient analysis.

Figure 1 illustrates the geometry of an interface between head and tape typical of $\frac{1}{2}$ -inch (1.27 cm) tape drives in computer systems. It is generally assumed that the width of the head and tape is sufficiently large to inhibit side flow in the air-bearing region; thus, the unknowns are defined as functions of a single spatial coordinate. The quantity that is generally of most interest in such problems is the steady-state separation between the head and the tape, dependent on the head shape and on a host of parameters describing the medium and the air film. To obtain the solution of this problem, previous investigators have derived the steady-state equations for the tape shape and for the air film in a coordinate system relative to the circular head, and have then solved the steady-state equations numerically to obtain the separation between head and tape.

The problem formulation and solution procedure presented in this paper differ from conventional foil-bearing theory in four respects. First, the equations of motion for the tape are not written relative to the head; instead, the undeflected tape (in the absence of the head) is used as a reference surface. Second, the inertial terms in the tape equation arising from the axial motion of the tape are retained in the analysis. Third, a finite segment of the

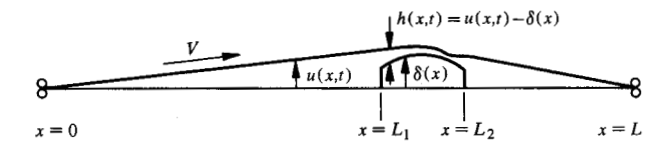


Figure 1 Geometrical aspects of the interface between head and tape in typical $\frac{1}{2}$ -inch (1.27 cm) tape drive.

tape with appropriate boundary conditions is considered, rather than the usual asymptotic foil boundary conditions. Finally, all time-dependent terms are retained in both the tape and lubrication equations. The solution then consists in prescribing some arbitrary initial conditions and numerically tracking the complete dynamic transient problem to the final steady-state solution.

For large penetrations of the head into the tape, the tape model, linearized on the assumption of small deflections, might be expected to predict the tape shape less accurately than does the usual foil-bearing theory. However, for tape deflections typical of tape-drive configurations, the model is expected to be adequate, and, moreover, offers the ability to analyze noncircular head geometries. In addition, we gain the ability to analyze wave-propagation effects in the axially moving tape and to analyze the interaction of waves in the tape with the air-bearing region.

Problem formulation

We consider a finite-length foil moving at constant velocity between two supports, as shown in Fig. 1. The deflection of the foil away from its equilibrium position is denoted by u(x, t). Swope and Ames [13] have derived the equations of motion for such a foil (disregarding flexural rigidity) and have presented numerous analytical results depicting wave-propagation effects, which will be referred to subsequently. An alternate derivation, including the effects of flexural rigidity, has been given by Mote [14]. We wish to retain flexural rigidity in the analysis and, hence, use that equation to describe the dynamics of the moving foil:

$$m(u_{tt} + 2Vu_{xt} + V^2u_{xx}) + du_t + EIu_{xxxx} - Tu_{xx}$$

= $p - p_x$, (1)

where m is the mass density of the foil per unit length, V the foil velocity, E the modulus of elasticity, I the moment of inertia of the cross section, T the tape tension, d a damping coefficient, p the force per unit length, and p_a the ambient pressure.

The force acting on the tape p(x, t) is the pressure developed in the air-bearing region $L_1 \le x \le L_2$. Outside of this region the pressure is taken to be ambient. The geometry of the head is described by $\delta(x)$, representing the penetration of the head past the equilibrium tape

position. The separation between the head and the tape is the region $L_1 \le x \le L_2$ is then

$$h(x,t) = u(x,t) - \delta(x), \qquad L_1 \le x \le L_2. \tag{2}$$

This separation is then used in the one-dimensional transient Reynolds equation to compute the pressure p(x, t) in the air-bearing region,

$$(h^3 p p_x)_x + 6 \lambda_a p_a (h^2 p_x)_x = 6 \mu V(ph)_x + 12 \mu(ph)_x,$$
 (3)

where λ_a is the mean free path length at ambient pressure p_a , and μ is the air viscosity. Thus, we retain terms corresponding to compressibility and slip flow in the transient Reynolds equation.

Boundary conditions for the problem are taken to be

$$u(0, t) = 0,$$
 $u_{xx}(0, t) = 0,$ (4) $u(L, t) = 0,$ $u_{xx}(L, t) = 0,$

and

$$p(x,t) = p_a$$
 for $0 \le x \le L_1$ and $L_2 \le x \le L$, (5)

that is, we assume simply supported boundary conditions for the tape and assume that the pressure is ambient at the edges of the head.

Initial conditions are taken as

$$u(x,0) = \bar{u}(x), \qquad p(x,0) = p_0,$$
 (6)

where $\bar{u}(x)$ is chosen so that h(x, 0) is positive valued in the range $L_1 \le x \le L_2$, and p_0 is a constant pressure, generally assumed to be above ambient pressure.

Numerical solution of equations

The system of equations (1)-(6) is solved by substituting difference operators for the derivative operators and then solving the resultant difference equations. To accomplish this, a uniform grid of mesh Δx is imposed on the spatial domain $0 \le x \le L$. The time domain is also made discrete by choosing a time step Δt . The coupling of Eqs. (1) and (3) through Eq. (2) is accomplished by solving the difference equation corresponding to Eq. (3) at a given time step, using the existing solution for Eq. (1), and then solving the difference equation corresponding to Eq. (1), using the new solution for Eq. (3). This process is repeated for successive time steps.

Consider Eq. (1) first. Let the space mesh points be indexed by i, where $i = 0, 1, 2, \dots, n$ and $L = n\Delta x$. Then, $u_i^j = u(i\Delta x, j\Delta t)$ is the value of u at the ith space point and jth time step. The difference approximations used are

$$\begin{split} u_{xx} &= (u_{i+1}^{j+1} - 2u_i^{j+1} + u_{i-1}^{j+1})/\Delta x^2, \\ u_{tt} &= (u_i^{j+1} - 2u_i^j + u_i^{j-1})/\Delta t^2, \\ u_{xt} &= (u_{i+1}^{j+1} - u_{i+1}^{j-1} - u_{i-1}^{j+1} + u_{i-1}^{j-1})/4\Delta x \Delta t, \\ u_{xxxx} &= (u_{i+2}^{j+1} - 4u_{i+1}^{j+1} + 6u_i^{j+1} - 4u_{i-1}^{j+1} + u_{i-2}^{j+1})/\Delta x^4. \end{split} \tag{7}$$

When these are substituted into Eq. (1) and like terms are collected, the following linear implicit difference equation results:

$$du_{i-2}^{j+1} + au_{i-1}^{j+1} + bu_{i}^{j+1} + cu_{i+1}^{j+1} + du_{i+2}^{j+1} = ep_{i}^{j+1} + F. \quad (8)$$

Here a, b, c, d, and e are constants independent of j derived from the mesh size $(\Delta x, \Delta t)$ and coefficients of Eq. (1), and F contains values of u for time steps j and j-1.

The pressure values p_i^{j+1} are obtained from the solution of the difference equation corresponding to Eq. (3), except for the space points that lie outside the range $L_1 \leq i\Delta x \leq L_2$. The value of p_i^{j+1} outside this range is taken to be the ambient pressure p_a . The values of u_{-1}^{j+1} , u_0^{j+1} , u_n^{j+1} and u_{n+1}^{j+1} are known and depend on the type of boundary condition imposed at the ends of the tape. Thus, the difference equations (8) form a qui-diagonal system of linear equations, in which the only nonzero terms of the coefficient matrix are located on the five main diagonals. This system can be solved very efficiently by a recursive technique. The solution at each time step is derived from the solution at the preceding two time steps. For j=1 the solutions for the preceding steps j=0 and j=-1 are both set equal to the assumed initial displacement f(x) of the tape. This is equivalent to the initial conditions

$$u(x, 0) = \bar{u}(x)$$
 and $u_{\epsilon}(x, 0) = 0$.

Equation (3) is treated in a similar way. The difference approximations used are

$$\begin{split} p_x &= (p_{i+1}^{j+1} - p_{i-1}^{j+1}) / 2\Delta x, \\ p_t &= (p_i^{j+1} - p_i^j) / \Delta t, \\ p_{xx} &= (p_{i-1}^{j+1} - 2p_i^{j+1} + p_{i+1}^{j+1}) / \Delta x^2, \\ h_x &= (h_{i+1}^j - h_{i-1}^j) / 2\Delta x, \\ h_t &= (h_i^j - h_i^{j-1}) / \Delta t, \\ h_i^j &= u_i^j - \delta(i\Delta x). \end{split}$$

If the above Eqs. (9) are substituted into Eq. (3), the resulting difference equation is not linear and thus is inconvenient to solve. The equation can be linearized by using an approximation at the old time step j instead of the new time step j+1 in those terms involving products of p and its derivatives. To see how this is done, consider the term $(h^3pp_x)_x$ in Eq. (3). The result after carrying out the differentiation is $3h^2h_x\bar{p}p_x + h^3\bar{p}_xp_x + h^3\bar{p}p_{xx}$. If p_i^j is used for \bar{p} instead of p_i^{j+1} and a difference approximation involving j instead of j+1 used for \bar{p}_x , then the result is linear in those values of p at time step j+1. The difference approximations for p and its derivatives are known quantities because they involve p at time steps p and p 1. The difference equation that results after the above linearization has the form

$$A p_{i-1}^{j+1} + B p_i^{j+1} + C p_{i+1}^{j+1} = G.$$
 (10)

Here A, B, C and G involve values of p at step j and values of h at steps j and j-1. With suitable boundary values, the difference equation (10) can be solved by solving a tri-diagonal system of linear equations by a recursive technique.

The accuracy with which the solution of the difference equations (8) and (10) represent the solution of (1) -(3) is difficult to determine. One indication of the accuracy is the discretization errors of the difference operators used. The difference formulas (7) give order Δx^2 and Δt^2 discretization errors for the space and time derivatives, respectively, while formulas (9) give order Δx^2 in the space derivatives but only order t in the time derivative. Another source of error is the "coupling error" which comes about because Eqs. (8) and (1) are solved independently at each time step. These equations were chosen because of their simplicity and ease of programming, although a penalty in computation efficiency is paid because of the requirement of a small Δt . It should be possible to achieve a higher order of accuracy in (10) by using the averaging technique of the Crank-Nicolson method.

In the results that follow, the appropriate space and time steps, Δx and Δt , were determined by numerical experiment. The most critical is the value of Δt . We found that the solution of the difference equations (8) and (10) was stable for values of Δt substantially larger than that required for accuracy. To determine a suitable value of Δt for a given choice of Δx , a "steady state" solution was calculated using a relatively large value for Δt . Next, the solution was continued for smaller Δt . If the steady state achieved in the first run changed substantially, the solution was continued for smaller Δt . In all cases only one or two refinements of Δt were necessary to find one which caused no further change in the steady state. Finally, the problem was rerun from the initial state using the value Δt as found above. In all cases the steady state obtained in the final run agreed with that obtained by Δt refinement.

The dependence of the steady-state solution on the time step for large values of Δt is evidently due to the technique used to couple the two equations numerically. This would not be anticipated if the equations are combined into a single partial differential equation before numerical solution, or if a more accurate coupling technique is utilized in place of the simple scheme used here.

Simulation results

To establish the validity of the finite-difference formulations and the solution procedure, the tape-motion equation (1) and the lubrication equation (3) were first solved separately without interaction and compared with known analytic solutions. A good correlation with exact solutions led to increased confidence that the interactive

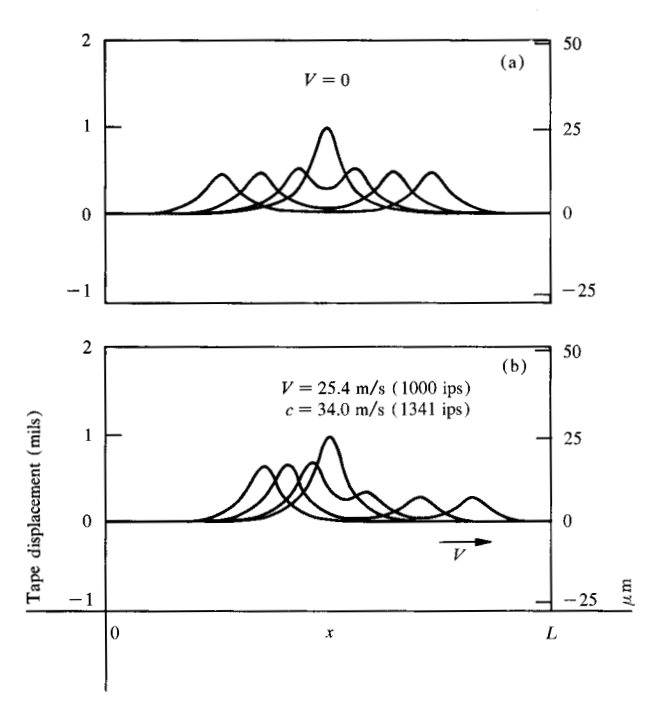


Figure 2 Numerical solutions for two cases of the wave propagation in a moving tape showing the motion of an initial disturbance. (a) Both tape and reference frame stationary. (b) Tape in axial motion relative to the reference frame.

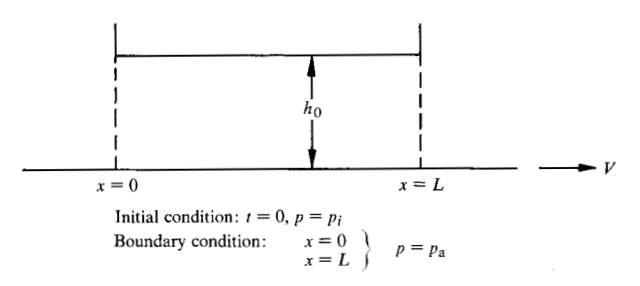
system could be solved. Results are first presented for the separate solutions, followed by examples of the interactive problem.

• Moving tape transient analysis

Because the tape is in axial motion relative to the reference frame, the observed transient vibration of the tape is somewhat different from that observed in a reference frame fixed relative to the tape. As an illustration of this, consider the motion of an initial disturbance in the tape shape as depicted in Fig. 2. Flexural rigidity is neglected to compare with the results of Swope and Ames [13]. At time t = 0, the tape is deformed into a "bump" shape in the center. The tape is then released, and the resulting transient motion is allowed to propagate through the medium. If both the tape and the reference frame are stationary, the bump separates into two similar bumps of equal amplitude ($\frac{1}{2}$ the amplitude of the original bump) moving in opposite directions at the same velocity, c = $\sqrt{T/m}$. If the tape is moving relative to a fixed frame, however, the wave-propagation velocities in opposite directions are different (c + v) and c - v in the positive and negative x directions, respectively). Further, the amplitudes of the disturbances are no longer equal. The high-speed disturbance has a lower amplitude than the low-speed disturbance, as the numerical solution shown in Fig. 2 indicates. Reference [13] contains a more detailed discussion of this type of transient behavior. If flexural rigidity is included in the analysis, the propagation velocities become wavelength dependent, and the resulting dispersion causes a change in the shape of the bumps as they move away from the initial state.

• Lubrication equation transient analysis

A special case of Eq. (3) must be considered to derive analytic results for comparison with the numerical solution. (We are not aware of any analytic solutions of the transient Reynolds equation that retain both compressibility and slip flow.) The problem solved here is that of parallel plane surfaces in relative motion. At time zero, the pressure is assumed to be uniformly higher than the ambient pressure along the entire bearing surface; the transient pressure decay to ambient is then calculated.



Even with h(x) assigned to be a constant h_0 , the differential equation (3) is still nonlinear in p(x). We can obtain an analytic solution only by linearizing the equation; the slip-flow term is also neglected for further simplification. Thus, the differential equation (3) becomes

$$(h^3 p_a p_x)_x = 6\mu V(ph)_x + 12\mu(ph)_t. \tag{11}$$

The solution to the linearized equation is

$$\frac{p(x, t) - p_{a}}{p_{i} - p_{a}} = \frac{\pi}{\Lambda} \sum_{n=1}^{\infty} \frac{n[1 + (-1)^{n+1} \exp(-\Lambda/2)]}{\frac{\Lambda}{8} + \frac{n^{2}}{2} \frac{\pi^{2}}{\Lambda}}$$

$$\times \exp(-\lambda t) \exp\left(\frac{\Lambda}{2} \frac{x}{L}\right) \sin(n\pi x/L),$$

where

$$\lambda = (V/L)[(\Lambda/8) + (n^2\pi^2/2\Lambda)],$$

$$\Lambda = 6\mu V L/p_a h^2.$$
(12)

These approximations imply that compressibility effects are small and that slip flow is negligible. Thus, it is expected that the analytic solution given above will be a very close approximation to the numerical solution of Eq. (3), providing the initial pressure differs only slightly from ambient, and that h_0 is sufficiently large so that slip flow is negligible. Numerical results from Eq. (3) are shown in Fig. 3. It was found that the analytic solu-

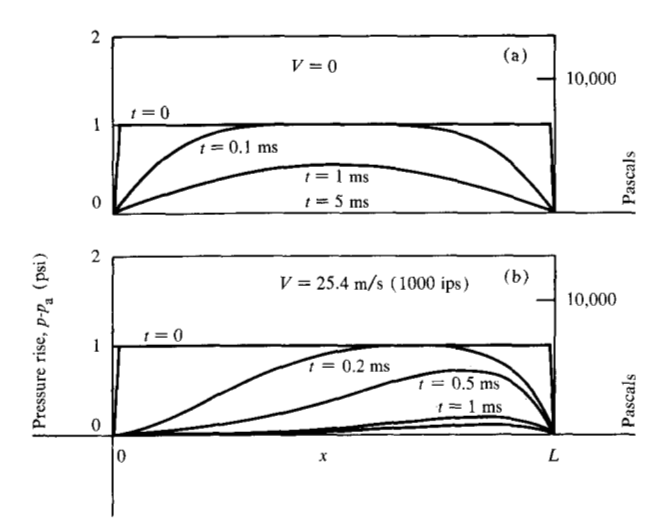


Figure 3 Numerical results from Eq. (3), showing transient pressure response between moving surfaces for cases (a) and (b) of Fig. 2.

tion and numerical solution are in nearly exact agreement, adding increased confidence in the transient finite difference solution of Eq. (3). As Fig. 3 indicates, when there is no relative motion between the two surfaces (V=0), the pressure symmetrically approaches the ambient value as t increases. With relative motion, the moving wall draws in the effect of the entrance boundary condition so as to reduce the pressure to the ambient value rapidly and asymmetrically.

• Coupled system equations

The initial concerns in attempting to solve the coupled system of transient equations were 1) whether the solution would converge to a steady-state solution, and 2) how well the steady-state solution would agree with conventional foil-bearing theory. Figure 4 illustrates the transient approach to steady state for a typical case, with a circular head of radius r in which the initial conditions are chosen from simple theory. (Table 1 lists the various parameters used for this figure; subsequent figures use the same parameters except as noted in the text.) The spacing between head and tape at time t=0 was taken to be a constant, equal to, in S. I. metric units,

$$h_0 = 0.0161r(6\mu V/T)^{\frac{2}{3}}$$

Ωī

0.643
$$r(6\mu V/T)^{\frac{2}{3}}$$
 in conventional units. (13)

The pressure at time t = 0 was also assumed to be constant:

$$p_0 = p_a + T/r. \tag{14}$$

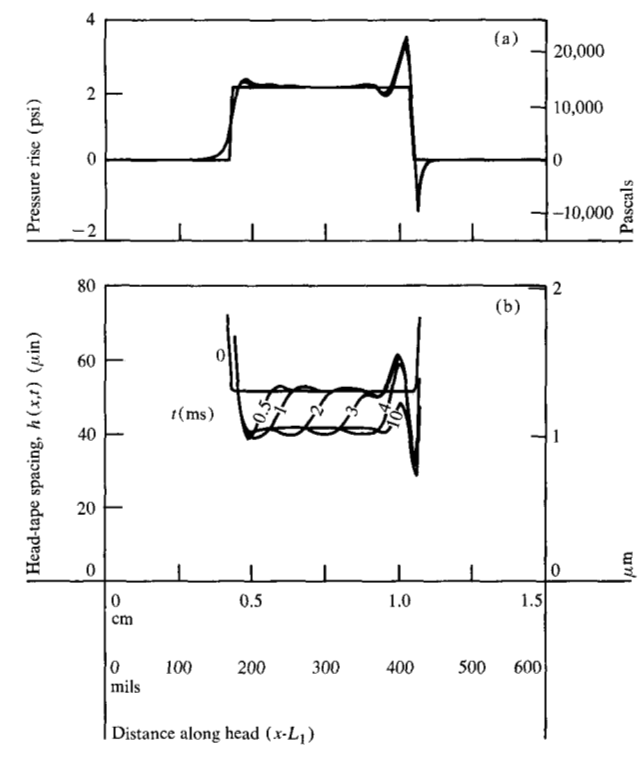


Figure 4 Development of steady-state solution based on coupled system of transient equations. (a) Solution for pressure over a circular head. (b) Solution for tape spacing over circular head.

Table 1 Simulation parameters, Figures 4-8.

```
Tape parameters:
                                  = 5.27 \times 10^{-4} \text{ kg/m} (2.95 \times 10^{-5} \text{ lb/in})
  m (density)
                                  = 1.52 \times 10^{-5} N-m (1.35 × 10^{-4} lb-in.)
= 1.78 \times 10^{-1} N/m (1.58 lb/in)
 EI (flexural rigidity)
  T (tension)
                                  = 2.54 \text{ m/s} (100 \text{ in./s})
   V (velocity)
Lubrication parameters:
                                   = 1.81 \times 10^{-4} poise (2.62)
   μ (viscosity)
                                      \times 10^{-9} \text{ lb-s/in.}^2
  P_a (ambient pressure) = 8.41 × 10<sup>4</sup> Pa (12.2 lb/in.<sup>2</sup>)
Head and tape geometry:
   L = 8.43 cm (3.320 in.)
  L_1 = 3.47 cm (1.365 in.)
  L_2 = 4.97 cm (1.955 in.)
 \delta(x) is a circular arc, radius r = 2.04 cm (0.804 in.)
  \delta_{\text{max}} = 0.635 \text{ cm } (0.250 \text{ in.})
Finite difference parameters:
 \Delta t = 5 \times 10^{-7} \text{ s}
 \Delta x = 0.127 \text{ mm } (0.005 \text{ in.})
```

With these initial conditions, a relatively mild transient response results because the steady-state solution is not far removed from the starting condition. The final spacing and pressure agree quite well with expected results from foil-bearing theory, even though the penetration of

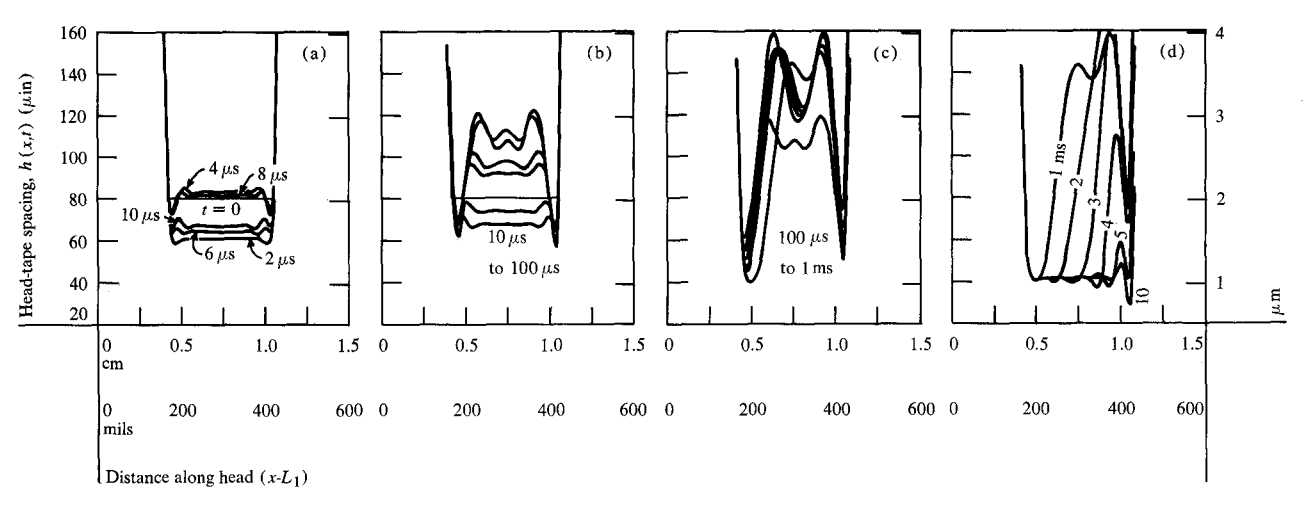


Figure 5 Development of steady-state solution from initial conditions producing a squeeze film transient. (a) to (d) Tape spacing over head for various time intervals.

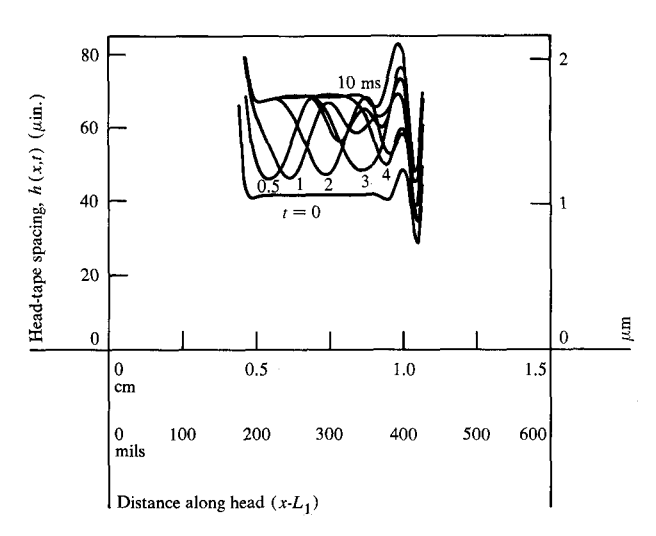


Figure 6 Dynamic response of the system due to a sudden reduction of tension. Data are for tape spacing over head.

the head into the tape is relatively large [0.635 cm (0.25 in.) or 6000 times the final uniform spacing of ≈ 1.07 μ m (42 μ in.)] The final spacing in the uniform region is smaller than the initial condition given by Eq. (13) because of flexural rigidity and slip flow. Each of these effects serves to reduce the spacing by approximately $0.125 \mu m$ (5 $\mu in.$) for this case. If they are neglected [I = 0 in Eq. (1) and N = 0 in Eq. (3)], the steady-state spacing is calculated as 1.26 μ m (50.4 μ in.), approximately 0.025 μ m (1 μ in.) less than the classical spacing given by Eq. (13). This difference of approximately two percent from classical theory in the steady-state uniform spacing region is typical of cases that we have investigated to date. From a practical viewpoint, the difference is insignificant, because experimental results generally involve substantially greater errors. Recent data using

white-light interferometry indicate that the measured spacing for the case shown in Fig. 4 is approximately 10 percent less than the calculated value; however, this is probably within the range of experimental error. Further comparisons of steady-state results are presented in a separate paper in this issue [15].

The transient response shown in Fig. 4 also provides a comparison with existing dynamic foil-bearing theories. The wavefront that propagates through the bearing regions is seen to have a velocity of approximately 1.25 m/s (50 in./s), or $\frac{1}{2}V$, for this case. This is the same propagation velocity obtained from theoretical models that neglect the inertia of the foil. The initial conditions chosen for Fig. 4 were sufficiently close to the actual steady-state solution that tape inertia effects were not an important factor in the transient response in this case.

Choice of initial conditions that depart markedly from the expected steady-state conditions can lead to very different transient response. For example, if we consider the previous case with the initial pressure set equal to ambient pressure, the transient response shown in Fig. 5 results. In this case, the tape moves rapidly toward the head because there are no pressure forces acting on the tape. This movement gives rise to a squeeze film that quickly builds up pressure to prevent the tape from contacting the head. The resulting pressure is more than sufficient to prevent contact, and a symmetric oscillatory squeeze film develops, having a period of approximately four μ s. After about 100 μ s the tape axial motion introduces some asymmetry into the spacing profile, and the resulting transient approach to steady state becomes quite complicated. After 10 ms the solution reaches the same steady-state condition as the previous case. The period of oscillation of this squeeze film and the nature

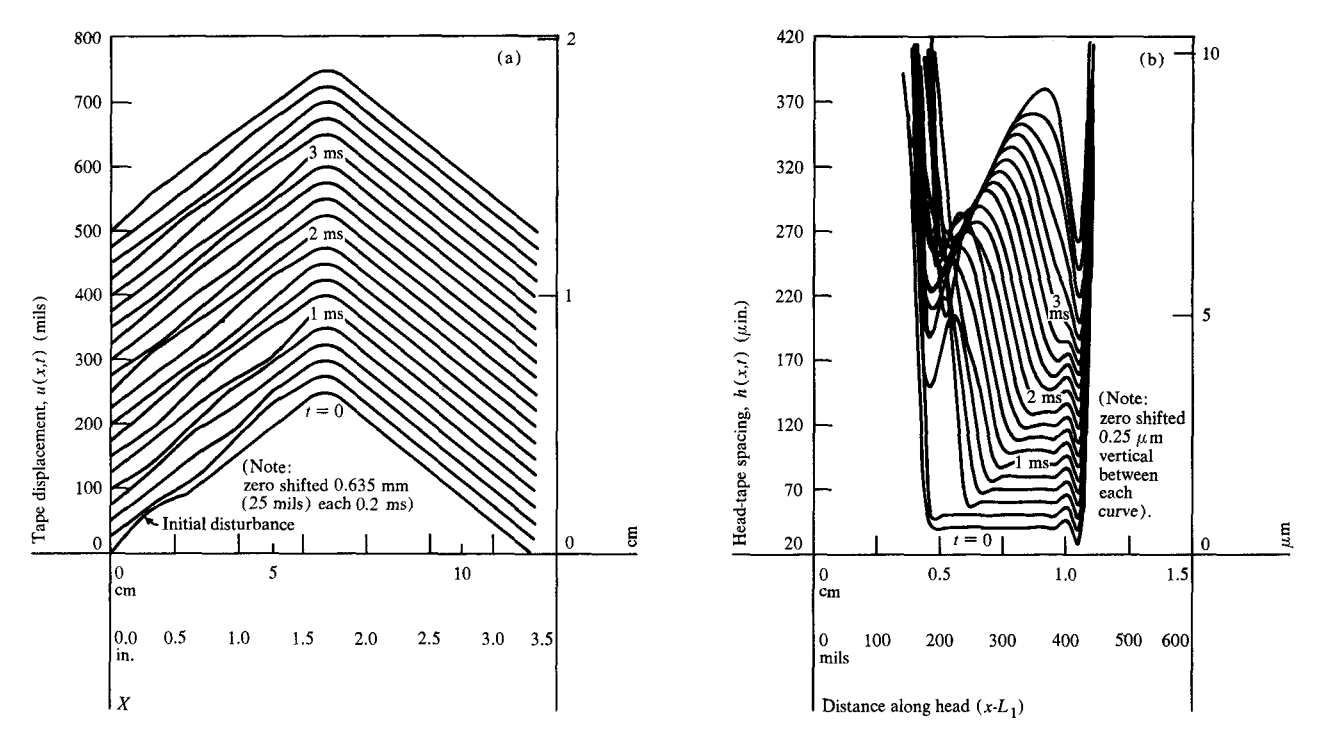


Figure 7 Computation at 0.2-ms intervals for wave reflection at the head when a wave is introduced in the tape. (a) Tape displacement. (b) Spacing over head.

of the subsequent transient response to steady state are dependent on the foil density and cannot be predicted by massless foil theories.

It is apparent from these results that the choice of a suitable time-step to model the transient behavior depends significantly on the nature of the response. If squeeze film effects are important, then a small time-step is required to simulate this behavior; otherwise, a larger time-step will adequately describe the system response. In the case of Fig. 4, a time-step of 0.5 μ s was used, and no significant changes in spacing were noticeable in the computed values after 10 ms. Thus, 20 000 iterations were required to reach steady-state conditions. The number of iterations and the total computer time (about five minutes on an IBM 370/195) to reach the steadystate solution are significantly smaller than we have been able to achieve by other methods, such as relaxation of the steady-state versions of Eqs. (1) and (3). Thus, it has been our experience that tracking the dynamic solution to steady state is more efficient computationally than attempting to solve the steady-state equations directly.

In addition to achieving the greater efficiency in deriving steady-state spacing and pressure profiles, the transient finite-difference approach is immediately usable for the investigation of many interesting problems involving coupled dynamics of the tape and air bearing. Having reached a steady-state condition, any of the system pa-

rameters can be perturbed to study dynamic interactions. For example, Fig. 6 illustrates the dynamic response of the system due to a sudden reduction of the tension; the steady-state solution from Fig. 4 was used as the starting condition.

Other transient conditions of interest involve the dynamics of the tape away from the head, and the interaction of waves in the tape with the air bearing. For example, the relative stability of various head configurations can be investigated by introducing a wave in the tape and observing the details of the wave reflection at the head. In Fig. 7, the steady-state solution from Fig. 4 is again used as an initial condition for such a case. At t = 0, the steady-state tape shape is perturbed by adding a sine wave of amplitude α and wavelength λ at the tape leading edge. For this particular choice of parameters, the propagation velocity of the disturbance in the tape is approximately $\sqrt{T}/m = 116 \text{ m/s} (4550 \text{ in./s}).$ Thus, the disturbance reaches the head and completes its first reflection in about 350 μ s. The wave in the tape reflects with opposite sign, as is typical of waves in a string reflecting off a pinned boundary. As the wave arrives at the head leading edge, the tape lifts abruptly, creating a sharp disturbance, which then begins to propagate through the air-bearing region. The propagation velocity in the air-bearing region is approximately V/2 =1.25 m/s (50 in./s), much lower than the tape wave speed. Before the disturbance has progressed through

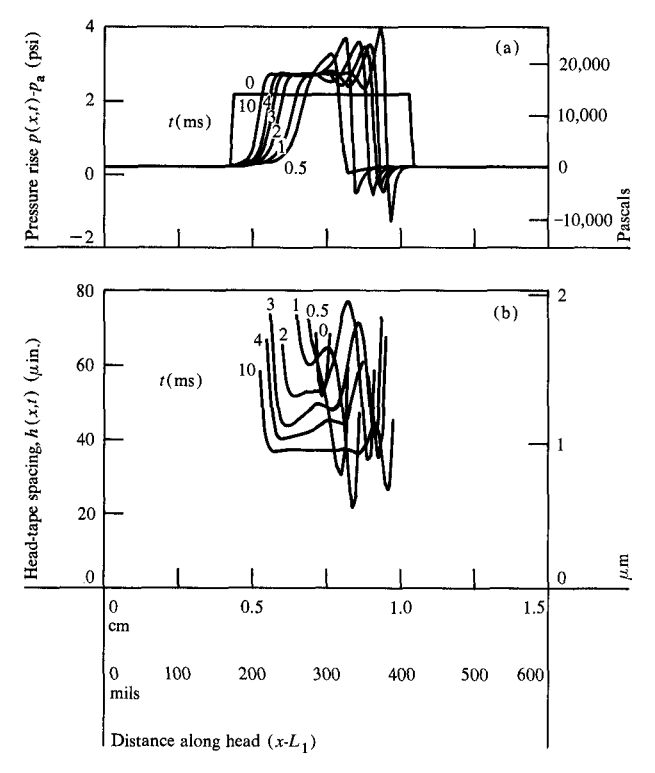


Figure 8 Solution for the case of a half-cycle, sine-wave head geometry. (a) Pressure over head. (b) Tape spacing over head.

the bearing, the wave in the tape thus has sufficient time to traverse back down the tape, reflect off the leading boundary, and traverse back to disturb the bearing region once again. Figure 7 shows that the initial disturbance has still not been transmitted by the air-bearing region by the time the fifth incident wave disturbs the inlet region. Parameters of interest in such a simulation include minimum and maximum spacing between head and tape during the interaction, and the transmissibility of air-bearing design (e.g., the propagation of the incident disturbance transmitted through the bearing region).

Noncircular head surfaces may be easily investigated. As a final example, a half-cycle, sine-wave head shape is chosen to closely resemble that of the circular head in Fig. 4, such that $\delta(L_1)$, $\delta(L_2)$, and the maximum penetration $\delta_{\rm max}$ are identical. Initial conditions are identical to Fig. 4 as well. Figure 8 illustrates the solution of this initial value problem. The locally smaller radius of curvature results in a lower, and shorter, region of uniform spacing than the circular head, and the pressure rise is somewhat greater.

Conclusions

The techniques utilized here appear to offer greater flexibility than conventional foil-bearing theory in the analysis of head-to-tape interfaces of the type shown in Fig. 1. First, the choice of reference frame simplifies the equations of motion, permitting an analysis of complex head shapes and allowing the incorporation of tape inertial properties generally neglected in foil-bearing theory. Second, obtaining the steady-state solution as the limiting case of an initial value problem is advantageous, even if the steady-state solution is all that is desired. Uniqueness of steady-state solutions to nonlinear equations, and the stability of these solutions, is of particular concern if the equilibrium state is found from the steadystate equations alone. Incorporating the time-dependent terms and solving the transient problem alleviates this concern. Finally, the ability to investigate dynamic interactions of wave propagation in the tape with the airbearing region is expected to provide many new insights into the transient behavior of foil bearings. Comprehensive results in this area have not yet been generated but will be explored in future work.

References

- E. J. Barlow; "Derivation of Governing Equations for Self-Acting Foil Bearings," J. Lubr. Technol., Trans. ASME 89, 334 (1967).
- E. J. Barlow, "Self-Acting Foil Bearings of Infinite Width," J. Lubr. Technol., Trans. ASME 89, 341 (1967).
- 3. M. Wildmann, "Foil Bearings," J. Lubr. Technol., Trans. ASME 90, 242 (1968).
- 4. W. E. Langlois, "The Lightly Loaded Foil Bearing at Zero Angle of Wrap," *IBM J. Res. Develop.* 7, 112 (1963).
- A. Eshel, "On Controlling the Film Thickness of Self-Acting Foil Bearings," J. Lubr. Technol., Trans. ASME 91, 359 (1970)
- A. Eshel and N. B. Elrod, "Stiffness Effects on the Infinitely Wide Foil Bearing," J. Lubr. Technol., Trans. ASME 89, 92 (1967).
- 7. J. T. S. Ma, "An Investigation of Self-Acting Foil Bearings," J. Basic Eng., Trans. ASME 87, 837 (1965).
- 8. A. Eshel and M. Wildmann, "Dynamic Behavior of a Foil in the Presence of a Lubricating Film," J. Appl. Mech., Trans. ASME 35, 242 (1968).
- 9. A. Eshel, "The Propagation of Disturbances in the Infinitely Wide Foil Bearing," J. Lubr. Technol., Trans. ASME 91, 120 (1969).
- A. Eshel, "Compressibility Effects on the Infinitely Wide, Perfectly Flexible Foil Bearing," J. Lubr. Technol., Trans. ASME 90, 221 (1968).
- 11. L. Licht, "An Experimental Study of Elastohydrodynamic Lubrication of Foil Bearings," J. Lubr. Technol., Trans. ASME 90, 199 (1968).
- 12. T. B. Barnum and H. G. Elrod, "A Theoretical Study of the Dynamic Behavior of Foil Bearings," J. Lubr. Technol., Trans. ASME 93, 133 (1971).
- 13. R. D. Swope and W. F. Ames, "Vibrations of a Moving Threadline," J. Franklin Inst. 275, 36 (1963).
- 14. C. D. Mote, "A Study of Band Saw Vibrations," J. Franklin Inst. 279, 430 (1965).
- 15. S. M. Vogel and J. L. Groom, "White-Light Interferometric Study of Elastohydrodynamic Lubrication of Foil Bearings," *IBMJ. Res. Develop.* 18, 521 (1974, this issue).

Received April 17, 1974

The authors are located at the IBM General Products Division Laboratory, Monterey and Cottle Roads, San Jose, California 95193.